Available online at www.sciencedirect.com
SCIENCE DIRECT®
International Journal of Thermal Sciences 44 (2005) 726–734
International Journal of Thermal Sciences
www.elsevier.com/locate/ijts

Mol solution for transient turbulent flow in a heated pipe ☆

Ahmet B. Uygur, Tanıl Tarhan, Nevin Selçuk *

Department of Chemical Engineering, Middle East Technical University, 06531 Ankara, Turkey

Received 10 August 2004; received in revised form 23 November 2004; accepted 4 January 2005

Available online 19 March 2005

Abstract

A computational fluid dynamics (CFD) code, based on direct numerical simulation (DNS) and method of lines (MOL) approach previously developed for the prediction of transient turbulent, incompressible, confined non-isothermal flows with constant wall temperature was applied to the prediction of turbulent flow and temperature fields in flows dominated by forced convection in circular tubes with strong heating. The code was parallelized in order to meet the high grid resolutions required by DNS of turbulent flows. Predictive accuracy of the code was assessed by validating its steady state predictions against measurements and numerical results available in the literature. Favorable comparisons obtained reveal that the code provides an efficient algorithm for DNS of non-isothermal turbulent flows.

Keywords: Direct numerical simulation (DNS); Non-isothermal flows; Method of lines (MOL); Turbulent flows; Transient flows

1. Introduction

Continuous advances in large scale computers, numerical methods and post-processing environments over the past two decades have led to the application of Direct Numerical Simulation (DNS), which is the most accurate and straightforward technique, to the prediction of turbulent flow fields. However due to the fact that fine space and time resolutions are needed for DNS, both accurate and efficient numerical techniques and high performance computers are required for the simulation in short computation time. The former can be achieved by increasing the order of spatial discretization method, resulting in high accuracy with less grid points, and using not only highly accurate but also a stable numerical algorithm for time integration. The method of lines, the superiority of which over finite difference method had already been proven [1], is an alternative approach that meets this requirement for the time dependent problems. The latter requirement is met by either supercomputers or parallel computers which require efficient parallel algorithms.

In the MOL approach, the system of partial differential equations (PDEs) is converted into an ordinary differential equation (ODE) initial value problem by discretizing the spatial derivatives together with the boundary conditions using a high order scheme and integrating the resulting ODEs using a sophisticated ODE solver which takes the burden of time discretization and chooses the time steps in such a way that maintains the accuracy and stability of the evolving solution. The most significant advantage of MOL approach is that it has not only the simplicity of the explicit methods but also the superiority of the implicit ones unless a poor numerical method for the solution of the ODEs is employed. MOL has been used extensively to solve PDEs since its first appearance in the former Soviet Union in 1930 and has been successfully applied to the solution of Navier–Stokes equations in both vorticity-stream function and primitive variables form. Considering the emphasis on the prediction of transient turbulent flows, a new CFD code satisfying the abovementioned requirements was recently developed for the DNS of 2D incompressible separated internal flows in regular and complex geometries. The code

☆ A preliminary version of this paper was presented at CHT-04: An ICHMT International Symposium on Advances in Computational Heat Transfer, April 2004, G. de Vahl Davis and E. Leonardi (Eds.) CD-ROM Proceedings, ISBN 1-5670-174-2, Begell House, New York, 2004.

* Corresponding author: Tel.: +90-312-210-2603; fax: +90-312-210-1264.

E-mail address: selcuk@metu.edu.tr (N. Selçuk).

1290-0729/$ – see front matter
doi:10.1016/j.ijthermalsci.2005.01.005

Nomenclature

c_p	specific heat capacity	$cm^2 \cdot K^{-1} \cdot s^{-2}$	
D	diameter	cm	
g	gravitational acceleration	$cm \cdot s^{-2}$	
i	grid index in r direction		
j	grid index in z direction		
k	thermal conductivity	$gr \cdot cm \cdot s^{-3} \cdot K^{-1}$	
L	length of the pipe	cm	
$\dot{m}$	mass flow rate	$gr \cdot s^{-1}$	
NR	number of grid points in r direction		
NZ	number of grid points in z direction		
p	pressure	$gr \cdot cm^{-1} \cdot s^{-2}$	
q^+	dimensionless heating rate		
r	distance in radial direction	cm	
Re	Reynolds number		
t	time	s	
t_p	user defined print time	s	
Δt	time step	s	
T	temperature	K	
u	axial component of the velocity	$cm \cdot s^{-1}$	
v	radial component of the velocity	$cm \cdot s^{-1}$	
z	distance in axial direction	cm	

Greek letters

ρ	density	$gr \cdot cm^{-3}$
ν	kinematic viscosity	$cm^2 \cdot s^{-1}$
ϕ	dependent variable transformed into 1D array	

Subscripts

in	inlet
max	maximum
NEQN	number of equations
w	wall

Superscripts

n	present time level

uses the MOL approach in conjunction with (i) an intelligent higher-order multidimensional spatial discretization scheme which chooses biased-upwind and biased-downwind discretization in a zone of dependence manner (ii) a parabolic algorithm which removes the necessity of iterative solution on pressure and solution of a Poisson type equation for the pressure (iii) an elliptic grid generator using body-fitted curvilinear coordinate system for application to complex geometries. Predictive accuracy of the code was assessed on various laminar and turbulent isothermal flow problems by validating its predictions against either measurements or numerical results available in the literature [2,3]. Favorable comparisons were obtained on these isothermal problems. First application of the code to a non-isothermal problem was the simulation of flow and temperature fields of a suddenly started laminar flow in a pipe with sudden expansion with hot wall at uniform temperature [4]. Although the results showed expected trends, validation of the code was not possible due to the absence of data.

Considering the interest in numerical simulation of transient turbulent non-isothermal flows in advanced power reactors, gas turbines, heat exchangers etc., the predictive accuracy of the code is tested by applying it to the simulation of turbulent, non-isothermal, axisymmetric flow of air through a strongly heated pipe for which experimental data are available on two entry Reynolds numbers and three different heating rates yielding conditions considered to be turbulent, sub-turbulent and laminarizing [5]. In order to meet the extensive grid requirement of DNS of turbulent flows, the code was parallelized by using domain decomposition strategy. To the authors' knowledge, a parallel implemented DNS code based on MOL for turbulent non-isothermal flows is not available to date.

2. Governing equations

The Navier–Stokes equations for transient two-dimensional incompressible non-isothermal flows in cylindrical coordinates are as follows:

continuity:

$$\frac{\partial u}{\partial z} + \frac{v}{r} + \frac{\partial v}{\partial r} = 0 \tag{1}$$

z-momentum:

$$\frac{\partial u}{\partial t} + u\frac{\partial u}{\partial z} + v\frac{\partial u}{\partial r} = -\frac{1}{\rho}\frac{\partial p}{\partial z} + \nu\left(\frac{\partial^2 u}{\partial r^2} + \frac{1}{r}\frac{\partial u}{\partial r} + \frac{\partial^2 u}{\partial z^2}\right) + \frac{1}{\rho}\left(\frac{\partial v}{\partial z} + \frac{\partial u}{\partial r}\right)\frac{\partial \mu}{\partial r} + \frac{2}{\rho}\left(\frac{\partial u}{\partial z}\right)\frac{\partial \mu}{\partial z} + g_z \tag{2}$$

r-momentum:

$$\frac{\partial v}{\partial t} + u\frac{\partial v}{\partial z} + v\frac{\partial v}{\partial r} = -\frac{1}{\rho}\frac{\partial p}{\partial r} + \nu\left(\frac{\partial^2 v}{\partial r^2} + \frac{1}{r}\frac{\partial v}{\partial r} - \frac{v}{r^2} + \frac{\partial^2 v}{\partial z^2}\right) + \frac{2}{\rho}\left(\frac{\partial v}{\partial r}\right)\frac{\partial \mu}{\partial r} + \frac{1}{\rho}\left(\frac{\partial v}{\partial z} + \frac{\partial u}{\partial r}\right)\frac{\partial \mu}{\partial z} + g_r \tag{3}$$

energy:

$$\frac{\partial T}{\partial t} + u\frac{\partial T}{\partial z} + v\frac{\partial T}{\partial r} = \frac{k}{\rho c_p}\left(\frac{\partial^2 T}{\partial r^2} + \frac{1}{r}\frac{\partial T}{\partial r} + \frac{\partial^2 T}{\partial z^2}\right) + \frac{1}{\rho c_p}\left(\frac{\partial T}{\partial r}\right)\frac{\partial k}{\partial r} + \frac{1}{\rho c_p}\left(\frac{\partial T}{\partial z}\right)\frac{\partial k}{\partial z} \tag{4}$$

The abovementioned equations are solved using the following boundary conditions:

$$\begin{aligned}
&\text{IC:} \quad @t=0,\ \forall z \wedge \forall r;\ u=0,\ v=0,\ T=T_{\text{in}}\\
&\text{BC1:}\ @r=0,\ \forall z \wedge \forall t;\ \partial u/\partial r=0,\ v=0,\ \partial T/\partial r=0\\
&\text{BC2:}\ @r=R,\ \forall z \wedge \forall t;\ u=0,\ v=0,\ T=T_w\\
&\text{BC3:}\ @z=0,\ \forall r \wedge \forall t;\ u=u_{\text{in}},\ v=0,\ T=T_{\text{in}}\\
&\text{BC4:}\ @z=L,\ \forall r \wedge \forall t;\\
&\quad \partial^2 u/\partial z^2=0,\ \partial^2 v/\partial z^2=0,\ \partial^2 T/\partial z^2=0
\end{aligned} \tag{5}$$

in which BC1, BC2 and BC3 represent axial symmetry, no slip condition at the wall and specified velocity and temperature profiles at the inlet, respectively. BC4 describes the developing flow also known as the soft boundary condition.

3. Numerical solution technique

This study is based on the assessment of the predictive performance of a novel CFD code based on MOL, for DNS of transient non-isothermal internal flows. In fact, many existing numerical algorithms can be considered as MOL algorithms. What differs MOL approach from the conventional methods is that, in the MOL approach higher-order, implicit and hence stable numerical algorithms are used for time integration. For the numerical solution of the same system of PDEs, the MOL approach and the conventional methods in which a lower-order either explicit or implicit time integration methods are used have the same system of ODEs as a result of spatial discretization. Therefore stability of the ODE problem, which can only be achieved by a scheme-adaptive spatial discretization of the convective terms in a zone of dependence manner, should be satisfied not only for the MOL approach but also for the conventional methods [6]. However, it should be noted that, satisfaction of the ODE stability criteria does not necessarily mean that the final solution as a result of time integration will also be stable. Thus to obtain overall stability and accuracy, first, one must satisfy ODE problem stability and second, use sophisticated (higher order, implicit) time integration methods. In this study, former is provided by employing a higher-order intelligent spatial discretization scheme of Oymak and Selçuk [6], and latter, time integration, is achieved by utilizing a quality ODE solver.

3.1. Higher order intelligent spatial discretization scheme

Spatial derivatives of dependent variables are approximated by using a five-point Lagrange interpolation polynomial which makes it possible to investigate the solutions of the governing equations by a higher order discretization scheme on both uniform and non-uniform grid topology. As it is well known, while discretizing the spatial derivatives, convective terms should be handled with extra care such that resulting system of ODEs should be stable according to the linear stability theory [7]. In the present code, this is achieved by using a multidimensional intelligent scheme which is based on the choice of biased-upwind or biased-downwind stencils for the convective derivatives according to the sign of the coefficient of the associated derivative [6].

3.2. Time integration

Substitution of the approximate expressions for the spatial derivatives into the governing equations yields the following set of ODEs in time:

$$\frac{\mathrm{d}\bar{\phi}}{\mathrm{d}t} = f(\bar{\phi}), \quad \bar{\phi} = (\phi_1, \phi_2, \ldots, \phi_{\text{NEQN}}) \tag{6}$$

Since the accuracy of the time integration scheme as well as the spatial discretization scheme is very important in essentially unsteady flows, the resulting system, with suitable initial and boundary conditions, is integrated by a quality ODE solver. Tests carried out with different ODE solvers, such as LSODES from the LSODE family [8] and ROWMAP [9] which is a Krylov-W code for the integration of stiff initial value problems, revealed that the latter is less CPU intensive than the former, a finding which has also been reported in a recent study carried out by Tarhan and Selçuk [10].

3.3. Pressure treatment and computation of radial velocity component

Computation of pressure is the most difficult and time-consuming part of the overall solution of the incompressible Navier–Stokes equations and involves the iterative procedure between the velocity and pressure fields through the solution of a Poisson-type equation for pressure to satisfy the global mass flow constraint and divergence-free condition for confined incompressible flows. Therefore in this study, a non-iterative procedure for the calculation of pressure as suggested by Raithby and Schneider [11] and Patankar and Spalding [12] and applied by Oymak and Selçuk [13] was used. Based on this approach, streamwise pressure gradient is calculated by the equation

$$\left(\frac{\partial \hat{p}}{\partial z}\right)_j^n = \frac{2\pi\rho \int_0^R \Phi_{i,j}^n r\,\mathrm{d}r - \dot{m}}{\pi R^2 \Delta t} \tag{7}$$

where

$$\begin{aligned}
\Phi_{i,j}^n = u_{i,j}^n - \Delta t \Bigg\{ & u_{i,j}^n \left(\frac{\partial u}{\partial z}\right)_{i,j}^n + v_{i,j}^n \left(\frac{\partial u}{\partial r}\right)_{i,j}^n \\
& - \frac{\mu}{\rho}\left[\left(\frac{\partial^2 u}{\partial z^2}\right)_{i,j}^n - \frac{1}{r}\left(\frac{\partial u}{\partial r}\right)_{i,j}^n + \left(\frac{\partial^2 u}{\partial r^2}\right)_{i,j}^n\right]\Bigg\}
\end{aligned} \tag{8}$$

Here $\dot{m}$ is the mass flow rate prescribed as the inlet condition and R is the radius of the tube.

In the present investigation, in order to decrease the computation time, r-momentum equation (Eq. (3)) is not solved and instead r-component velocity is determined with

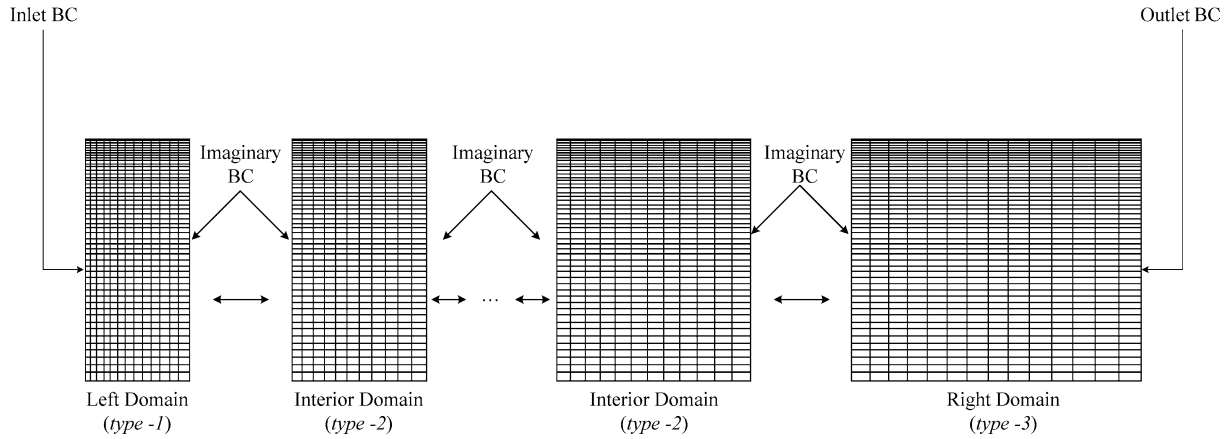

Fig. 1. Schematic representation of domain decomposition strategy.

the direct utilization of the continuity equation as suggested by Peyret and Taylor [14] and applied by Oymak and Selçuk [13]. By this approach, not only the r-component velocity is computed without bringing an extra burden on the code, but also divergence-free condition for incompressible flows is satisfied automatically. For this purpose the continuity equation is discretized and rearranged to yield

$$v^n_{i+1,j} = \frac{r_i}{r_{i+1}}\left[v^n_{i,j} - \Delta r_i^+ \left(\frac{\partial u}{\partial z}\right)^n_{i,j}\right] \tag{9}$$

where

$$i = 1, \ldots, NR-2,\ \ j = 2, \ldots, NZ,$$
$$\Delta r_i^+ = r_{i+1} - r_i \tag{10}$$

3.4. Parallel implementation

In order to meet the extensive grid requirement of DNS of turbulent flows, in this study, use has been made of an efficient parallel algorithm which can be executed on personal computer (PC) clusters.

For the parallel implementation of the serial code, domain decomposition technique by means of overlapping boundaries at the intergrid regions to provide information exchange between the sub-domains was used [15]. As a 5-point discretization scheme based on biased-upwind or biased-downwind stencils is utilized in this study, at least three points from the neighboring sub-domains are required to be exchanged. The algorithm is based on the master-slave paradigm, where the master process generates the grid structure, sets the initial and physical boundary conditions, decomposes the domain into sub-domains having the same number of grid points, sets the type of each sub-domain (*type*) and sends the related information to the slave processes. The type of sub-domain is determined according to the position of that sub-domain relative to the others (Fig. 1). The leftmost sub-domain is assigned as *type*-1, which includes an inlet boundary condition and an imaginary boundary condition; the rightmost sub-domain is assigned as *type*-3, which includes an imaginary condition and an outlet boundary condition; and the intermediate sub-domains are assigned as *type*-2, which include two imaginary boundary conditions. The slave processes perform the calculations for the sub-domains assigned to them according to the types set by the master process, advance in time and exchange necessary information between each other at user defined time steps (t_p) and send transient results to the master process for the development of the transient solution until steady state is reached. Parallel virtual machine (PVM) and two dual-processor (Pentium III) PCs connected via a 100 Mbps switch were used as message passing software and parallel computing platform, respectively.

4. Results

For the evaluation of the performance of the code, use has been made of the experimental data obtained by Shehata and McEligot [5] for turbulent flow and temperature fields in a pipe with strong wall heating, the only published internal profile data available to test general purpose CFD codes. Predictive ability and efficiency of the code was assessed by applying the code to the experimental rig of Shehata and McEligot and comparing its predictions with mean velocity and temperature measurements for three generic cases corresponding to turbulent, sub-turbulent and laminarizing. Performance of the present code with respect to that of another code from the literature was also demonstrated on the laminarizing case. Test case under consideration is described below.

4.1. Test case: Turbulent flow of air in a pipe with strong wall heating

The experimental objective of Shehata and McEligot [5] was to measure the mean streamwise velocity and temperature for dominant forced convection in a well-defined, axisymmetric experiment involving significant variation of the

gas transport properties across the viscous layer. The experiment was conducted in an open loop built around a vertical resistively heated circular test section exhausting directly to the atmosphere. The experiment was designed to approximate a uniform wall heat flux to air entering with a fully developed turbulent velocity profile at a uniform temperature ($T_{in} = 298$ K). Heated length was about 32 D ($D = 1.37$ cm) and it was preceded by 50 D unheated entry region for flow development. Details of the experiment and tabulated data is available in a report by Shehata and McEligot [16].

Experimental conditions were selected to correspond to three generic situations:

- Essentially turbulent flow with slight but significant air property variation;
- Severe air property variation evolving to near laminar flow;
- Moderate gas property variation yielding behavior that was intermediate or transitional between the first two.

The convention used for identifying the respective runs and their flow regimes are summarized in Table 1.

Table 1
Flow conditions

Run	Re_{in}	q^{+} [a]	Flow regime
618	6033	0.0018	Turbulent
635	6025	0.0035	Sub-turbulent
445	4240	0.0045	Laminarizing

[a] q^{+} is the dimensionless heat flux applied to the walls of the pipe and defined as, $q^{+} = q''_w/(\dot{m} c_{p_{in}} T_{in})$.

4.2. Grid structure and grid independency test

A grid system which is non-uniform in both radial and axial directions is utilized in the computations. Higher number of grid points are employed in the vicinity of the inlet and the wall to account for the sharp gradients occurring in these regions (Fig. 1).

Simulations with grid resolutions of 251×501, 351×501 and 501×901 in r and z directions, respectively, were carried out. The finest resolution is the one required by 2D DNS for the highest Reynolds number ($Re = 6000$) under consideration, which has been employed for the first time

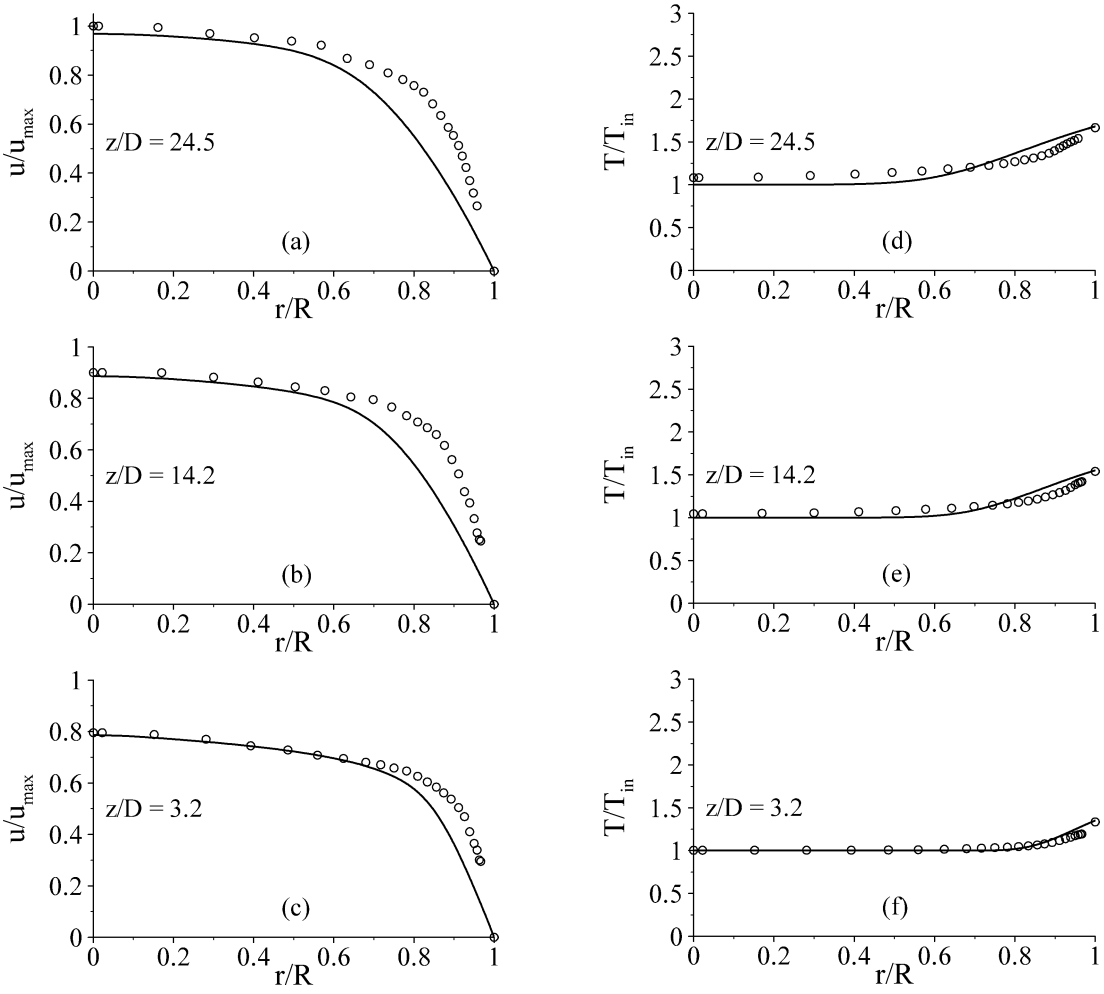

Fig. 2. Mean velocity and temperature profiles for Run 618: (a)–(c) velocity; (d)–(f) temperature. ○: experimental data [5]; —: present study.

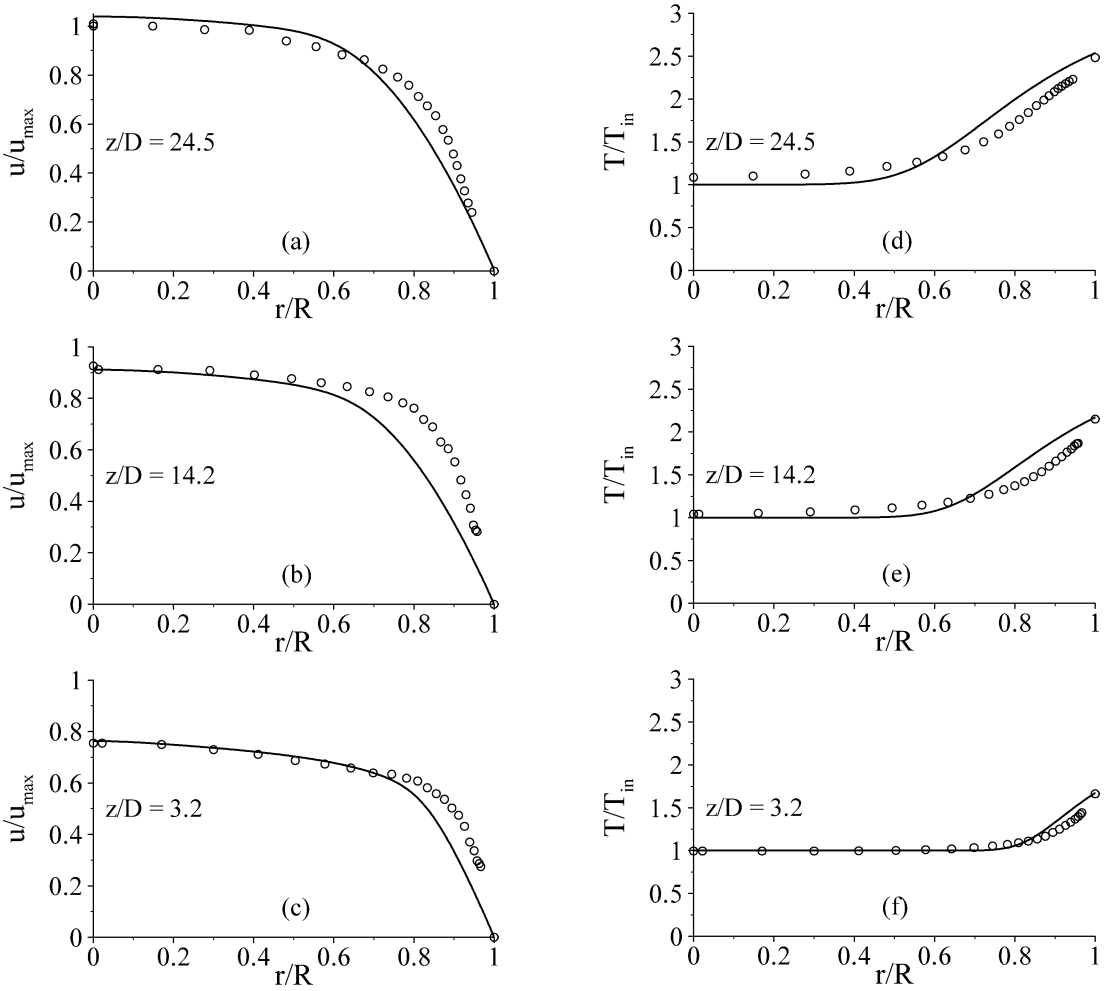

Fig. 3. Mean velocity and temperature profiles for Run 635: (a)–(c) velocity; (d)–(f) temperature. ○: experimental data [5]; —: present study.

since the development of the code. Comparison of the velocity and temperature profiles obtained with these different resolutions revealed that grid independent solutions can be obtained with much lower resolution (251×501) than that required by 2D DNS.

4.3. Steady state velocity and temperature profiles

In what follows, the predicted steady state axial velocity and temperature profiles at three axial locations along the pipe are validated against the measurements of Shehata and McEligot [5] for all runs and the numerical solution of Satake et al. [17] for Run 445.

4.3.1. Run 618 and Run 635

Comparisons of predicted and measured axial velocity and temperature profiles for Run 618 at three different axial locations, namely $z/D = 3.17$, 14.2 and 24.5, are illustrated in Fig. 2. Velocities are normalized by the maximum axial velocity observed in the measurements whereas temperatures are normalized by the inlet temperature T_{in}. As can be seen from Fig. 2(a)–(c), the velocities are predicted well in the core region and are underpredicted in the near wall region. This can be attributed to the uncertainty in measured values, reported to be in the range of 8–10% of the point value with larger percent uncertainties occurring near the wall. Among the three cross sections the best agreement is obtained at the first station. It can be noted that the velocity distributions at the first station appears to represent typical developed turbulent flow in a tube. As downstream stations are reached, the gradient at the wall decrease with progressive decrease in Reynolds number due to an increase in temperature and viscosity. Comparison between predicted and mean temperature at three different axial locations for Run 618 is presented in Fig. 2(d)–(f). As can be seen from the figure, predicted and measured temperature profiles are in excellent agreement. As flow progresses downstream, temperatures are overpredicted in the wall region and underpredicted in the core region. Interpreting this observation in terms of energy transport, the code predicts a lower rate of turbulent transport than observed from the wall region to the core; probably due to thickening of viscous layer at these stations.

The predicted and measured velocity and temperature profiles for Run 635 are illustrated in Fig. 3. With the ex-

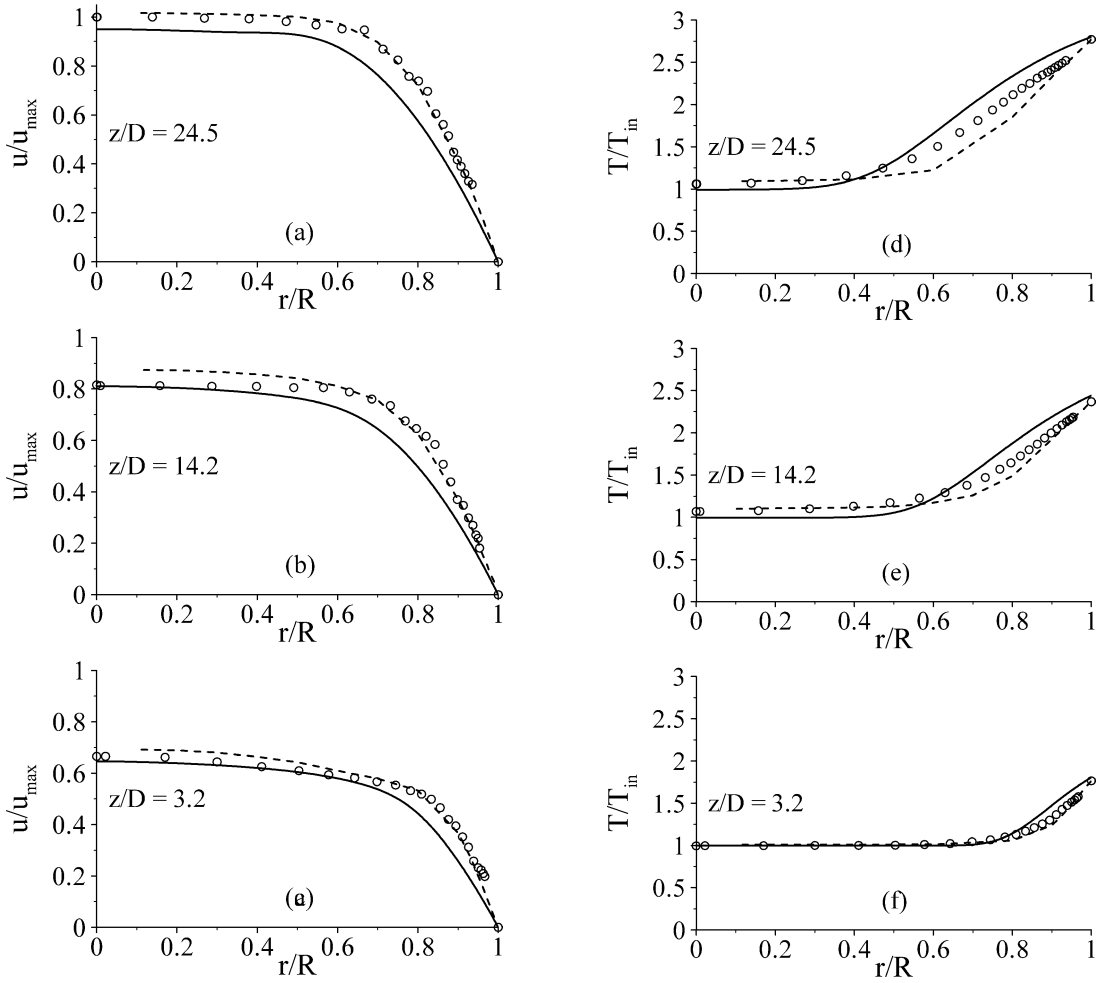

Fig. 4. Mean velocity and temperature profiles for Run 445: (a)–(c) velocity; (d)–(f) temperature. ○: experimental data [5]; - - - -: DNS by Satake et al. [17]; —-: present study.

ception observed at the last station ($z/D = 24.5$) for the velocity profiles, discussions carried out for Run 618 are also valid for Run 635. As can be seen in Fig. 3(a)–(c), the poorest agreement between the velocity profiles is obtained at $z/D = 14.2$ and the agreement tends to improve at $z/D = 24.5$. This trend has also been observed when RANS predictions obtained by Shehata and McEligot were compared with their measurements [5].

4.3.2. Run 445

The last set of the runs, Run 445, is at the highest heating rate ($q^+ = 0.0045$) and the lowest Reynolds number ($Re = 4240$). These conditions were categorized as being on the borderline between sub-turbulent and laminarizing flow by Shehata and McEligot [5]. Predictions of the present code were also compared with those of another DNS code available in the literature [17] for Run 445 (Fig. 4). Favorable comparisons are obtained in both cases.

An overall assessment of the performance of the code shows that the predictions for Run 445 are in better agreement with the measured data compared to the other two runs.

In order to demonstrate the predictive ability of the present code for the transient solutions, time development of velocity and temperature fields for Run 445 are illustrated in Fig. 5. Snapshots of the flow (a)–(e) and temperature (f)–(j) fields at different instances show the gradual transfer of heat from the wall to the fluid and the corresponding acceleration in the flow field (both displayed by contour color changing from blue to red). As a consequence of lowest Reynolds number ($Re = 4240$) and highest heating rate ($q^+ = 0.0045$) employed in this run, the boundary layer thickness at the exit of the pipe reaches approximately three fourths of the radius, resembling non-isothermal laminar pipe flow. However the same behavior is not observed in the flow field where a major portion of the profile is flat, exhibiting turbulent characteristics.

4.4. Performance of the parallel code

In parallel computing community, performance is often assessed in terms of speed-up and efficiency; speed-up being the ratio of the total execution time of the parallel code

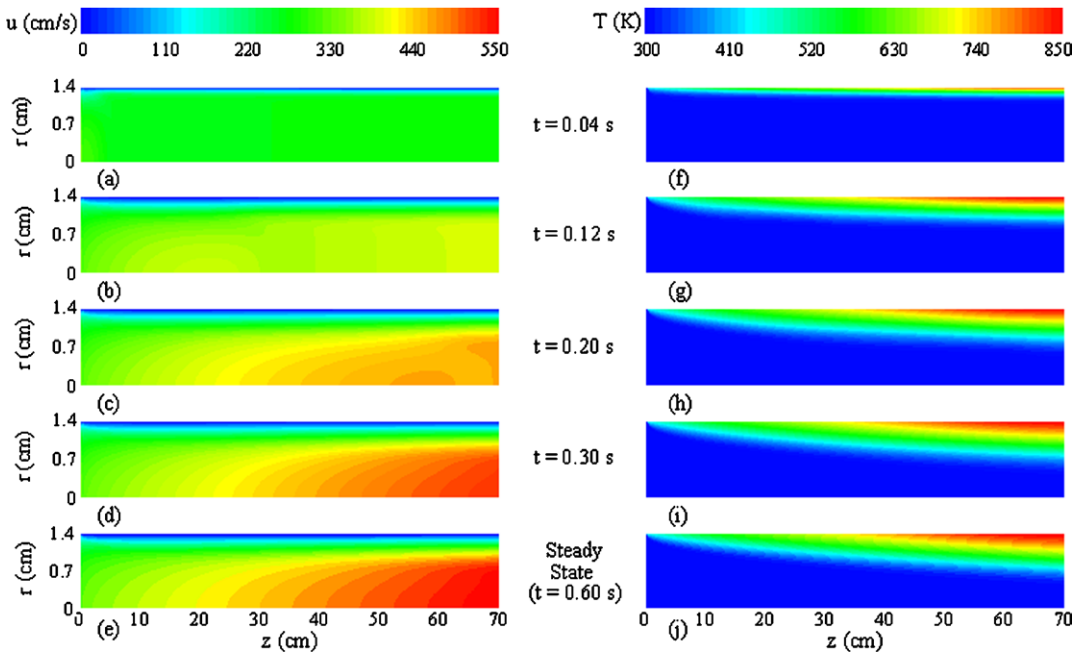

Fig. 5. Transient velocity and temperature field—Run 445: (a)–(e) velocity; (f)–(j) temperature.

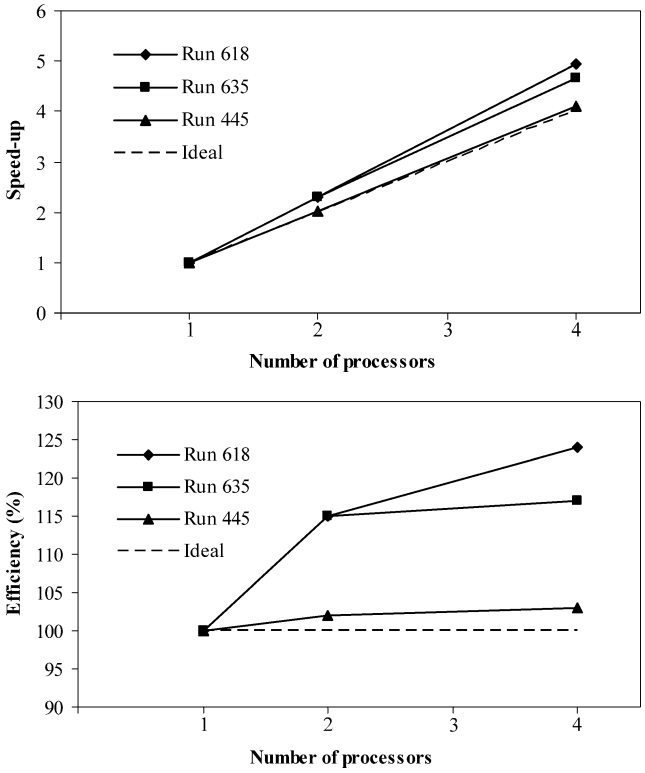

Fig. 6. Performance of the parallel code with respect to speed-up and efficiency.

to that of the serial one and efficiency being the ratio of the speed-up to the number of processors employed. In the ideal case, maximum speed-up and efficiency that can be observed are equal to the number of processors used in the execution and 100%, respectively. Fig. 6 displays the performance of the code in terms of abovementioned parameters. As can be seen from the figures, the speed-up and efficiency values obtained from the runs carried out with two and four processors exhibit super-linear trend, i.e., higher than the ones for the ideal case. This can be attributed to the insignificant communication delay between the sub-domains caused by the absence of sharp gradients in the test problem under consideration.

5. Conclusions

A CFD code, based on DNS and MOL approach for the prediction of transient turbulent, incompressible, confined non-isothermal flows with constant wall temperature was applied to the simulation of turbulent, non-isothermal, axisymmetric flow of air through a strongly heated pipe for which experimental data are available on two entry Reynolds number and three different heating rates yielding conditions considered to be turbulent, sub-turbulent and laminarizing. In order to meet the extensive grid requirement of DNS of turbulent flows, the code was parallelized by using domain decomposition strategy. On the basis of numerical experimentations the following conclusions were reached:

- The predicted velocity profiles are in good agreement with measurements in the core region and reasonable agreement is obtained in the vicinity of the wall. The overall agreement between predicted and measured temperature profiles was found to be better than that for velocity profiles.
- The predictive ability of the code is relatively better for lower Reynolds number turbulent flow.

- Predicted velocity and temperature profiles are in reasonably good agreement with other numerical results available in the literature.
- The code can meet the grid resolution requirement of 2D DNS. Owing to the stability and the efficiency of the algorithm, grid independent solutions can be obtained with much lower resolutions than the one required by 2D DNS.
- Super-linear speed-up and efficiency values can be obtained due to the reduced size of matrix computations on ODE solvers.

Encouraging agreement between predictions of the present code and measurements, the modularity of the code which enables the use of any higher order spatial discretization scheme and ODE solver and flexibility for incorporation of conservation equations for species and radiative energy place confidence in its further development and use.

References

[1] N. Selçuk, T. Tarhan, S. Tanrıkulu, Comparison of method of lines and finite difference solutions of 2D Navier–Stokes equations for transient laminar pipe flow, Internat. J. Numer. Methods Engrg. 53 (7) (2002) 1615–1628.

[2] N. Selcuk, O. Oymak, A novel code for prediction of transient flow field in a gas turbine combustor simulator, in: AVT Symposium on Gas Turbine Engine Combustion, Emissions and Alternative Fuels 12–16 October 1998, Lisbon, Portugal, NATO/RTO Meeting Proceedings 14, 11/1–10, 1999.

[3] T. Tarhan, N. Selçuk, Method of lines for transient flow fields, Internat. J. Comput. Fluid Dynamics 15 (2001) 309–328.

[4] O. Oymak, N. Selçuk, The method of lines solution of time dependent 2-D Navier–Stokes equations coupled with energy equation, in: G. de Vahl Davis, E. Leonardi (Eds.), Proceedings of the International Symposium on Advances in Computational Heat Transfer, Begell House, Çeşme, Turkey, 1997, pp. 256–264.

[5] A.-M. Shehata, D.-M. McEligot, Mean structure in the viscous layer of strongly heated internal gas flows. Measurements, Internat. J. Heat Mass Transfer 41 (1998) 4297–4313.

[6] O. Oymak, N. Selçuk, Transient simulation of internal separated flows using an intelligent higher-order spatial discretization scheme, Internat. J. Numer. Methods Fluids 24 (1997) 759–769.

[7] W.-E. Schiesser, The Numerical Method of Lines: Integration of Partial Differential Equations, Academic Press, New York, 1991.

[8] K. Radhakrishnan, A.-C. Hindmarsh, Description and use of LSODE, the Livermore solver for ordinary differential equations, Technical Report UCRL-ID-113855, Lawrance Livermore National Laboratory, NASA, 1993.

[9] E. Hairer, G. Wanner, Solving Ordinary Differential Equations II, Springer, New York, 1991.

[10] T. Tarhan, N. Selçuk, Numerical simulation of a confined methane/air laminar diffusion flame by the method of lines, Turkish J. Engrg. Environ. Sci. 27 (2003) 275–290, available online: http://journals.tubitak.gov.tr/engineering/issues/muh-03-27-4/muh-27-4-8-0303-2.pdf.

[11] G.-D. Raithby, G.-E. Schneider, Numerical solution of problems in incompressible fluid flow: Treatment of the velocity pressure coupling, Numer. Heat Transfer 2 (1979) 417–440.

[12] S.-V. Patankar, D.-B. Spalding, A calculation procedure for heat, mass and momentum transfer in three-dimensional parabolic flows, Internat. J. Heat Mass Transfer 15 (1972) 1787–1806.

[13] O. Oymak, N. Selçuk, Method of lines solution of time-dependent two-dimensional Navier–Stokes equations, Internat. J. Numer. Methods Fluids 23 (1996) 455–466.

[14] R. Peyret, T.-D. Taylor, Computational Methods for Fluids, Springer, New York, 1983.

[15] C. Erşahin, T. Tarhan, İ.-H. Tuncer, N. Selçuk, Parallelization of a transient method of lines Navier–Stokes code, Internat. J. Comput. Fluid Dynamics 18 (1) (2004) 81–92.

[16] A.-M. Shehata, D.-M. McEligot, Turbulence structure in the viscous layer of strongly heated gas flows, Idaho National Engineering Laboratory Technical Report INEL-95/0223, Idaho Falls, Idaho, 1995.

[17] S. Satake, T. Kunugi, A.-M. Shehata, D.-M. McEligot, Direct numerical simulation for laminarization of forced turbulent gas flows in circular tubes with strong heating, Internat. J. Heat Fluid Flow 21 (2000) 526–534.